

RESEARCH ARTICLE

A Consensus-Based Current Sharing Algorithm for Energy Storage Systems: An Application to Aeronautic Microgrids

GIACOMO CANCELLO¹, ANTONIO RUSSO², (Member, IEEE),
AND ALBERTO CAVALLO², (Member, IEEE)

¹Aeromechs, 81031 Aversa, Italy

²Dipartimento di Ingegneria, Università degli Studi della Campania “Luigi Vanvitelli,” 81031 Aversa, Italy

Corresponding author: Giacomo Cancelliello (giacomo.cancelliello@aeromechs.eu)

This work was partially funded under the selection notice issued by the Rector’s decree n. 509 of 13/06/2022 for the funding of fundamental and applied research projects dedicated to young researchers—ACTNOW and by the Italian Ministry of Universities and Research (MUR) under contract FSE-REACT-EU (Fondo Sociale Europeo-Assistenza alla Ripresa per la Coesione e i Territori d’Europa), PON (Programma Operativo Nazionale) Ricerca e Innovazione 2014–2020 DM1062/2021 and by the European Union under GA no 101101961 - HECATE. Views and opinions expressed are however those of the author(s) only and do not necessarily reflect those of the European Union or Clean Aviation Joint Undertaking. Neither the European Union nor the granting authority can be held responsible for them. The project is supported by the Clean Aviation Joint Undertaking and its Members.

ABSTRACT More Electric Aircraft (MEA) and All Electric Aircraft (AEA) require advanced autonomous electric Energy Management Systems (EMS) onboard the aircraft. The aircraft electric network can be considered as an islanded microgrid, and as such some approaches typical of the microgrid management can be used onboard the aircraft to design an effective EMS. In particular, distributed control with consensus techniques represents a promising approach due to the advantages in terms of reliability, computational simplicity and low-bandwidth requirement which are of great interest for implementation onboard. A consensus-based solution to the problem of coordinating and balancing several Energy Storage Systems (ESSs) coexisting in a generic aircraft architecture is proposed and analyzed. The proposed algorithm selects the current setpoints for each ESS according to their state of charge while ensuring safety of operations. Theoretical results and detailed simulations show the effectiveness of the proposed approach.

INDEX TERMS More electric aircraft, consensus, microgrid control, distributed control.

I. INTRODUCTION

Over the preceding two decades, extensive research has been dedicated to the examination of electric microgrids (MG) in the context of distributed electric energy management and distribution [1]. Specifically, researchers have focused their attention on the selection between direct current (DC) microgrids and alternating current (AC) microgrids. It is widely acknowledged that the majority of global electric distribution networks operate on AC current and voltages. The main reason for preferring AC to DC networks was the development of transformers at the end of the XIX century allowing simple step-up or step-down capabilities when using AC voltage. However, after one century this

motivation has been overcome by the development of electronic power converters, which allows the design of simple, cheap and efficient DC/DC converters. The development of this technology enables rethinking the electric distribution network as a DC network, with DC/DC converters as building blocks. There are several reasons for preferring DC MG to AC MG, e.g., most renewable sources produce DC power, many loads (LED, consumer electronics) employ DC power, classic Energy Storage Systems (ESS), like batteries and super-capacitors are DC devices [2]. However, there are still obstacles to the large-scale use of MG, often of economical or regulatory type: replacing the currently used AC infrastructure with DC MG has clearly a cost. However, if the size of the MG is limited the benefits of the DC solution are apparent. Indeed, from this point of view, islanded operations, where the MG is disconnected from the main network, have been addressed [3].

The associate editor coordinating the review of this manuscript and approving it for publication was Arturo Conde¹.

One application domain where limited-size MG can be employed is the transportation vehicles field. Each form of transportation vehicle has its own peculiarity. Notably, in the realm of terrestrial vehicles, critical considerations pertain to infrastructural interfaces with ground traffic and the optimal management of distributed loads [4]. Conversely, ships and aircraft represent distinct domains where islanded operations find particular relevance. For instance, ships necessitate the provision of substantial power within spatial constraints [5]. The aviation sector demands high levels of reliability, robustness, and effective load predictability capabilities [6]. This study is specifically centered on the formulation of an energy distribution strategy for MG systems within the aircraft domain.

A. THE ELECTRIC AIRCRAFT MG

In the context of aircraft electrification, an intermediate step towards the design of the All-Electric Aircraft (AEA) is the so-called More Electric Aircraft (MEA) [7], [8]. A pivotal challenge within the field of MEA lies in the substitution of hydraulic and pneumatic actuators with their electric counterparts. This substitution is aimed at enhancing system reliability, diminishing overall weights, and introducing novel functionalities in load control. Evidently, the expanded utilization of electric energy necessitates the implementation of new automated Energy Management Systems (EMS) onboard. The so-called “generic” architecture for the electric network of the aircraft, is a two-busbars system [9], [10] with a high voltage (HV) DC bus at 270V, a low voltage (LV) DC bus at 28V and a DC/DC bidirectional converter in between. The HV bus is energized by a starter-generator followed by a rectifier. On the HV side all the “heavy” loads are present (e.g., anti-icing, de-icing or electro-mechanic actuators), while on the LV side batteries are located, and also other ESS devices, like supercapacitors, are possible [11]. In conventional aircraft systems, typically one or two batteries are employed, contingent upon the aircraft’s size. These batteries function autonomously as starters for the engine or the Auxiliary Power Unit (APU), as well as providing power to essential loads in the event of engine failure [12]. Consequently, for a significant portion of their operational lifespan, batteries remain inactive. The implementation of automated ESS facilitates a more substantial utilization of batteries, for instance, during instances of overloads [9] or when prioritized loads necessitate power supply [13]. In recent developments, *structural batteries* [14] have emerged as devices with the dual capacity to store electric energy and provide structural support for mechanical loads. Their application holds promise for mitigating the weight-to-power density ratio of batteries, as these devices can serve as integral structural components. This prospect is particularly intriguing within aerospace systems and has already found practical implementation in unmanned aerial vehicles [15]. It is evident that structural batteries delineate a paradigm of multiple, distributed ESS, and their use necessitates the formulation of precise control strategies, especially in scenarios where

numerous ESS are concurrently deployed and their activities must be meticulously coordinated within a microgrid framework, as expounded upon in the subsequent section.

B. MG CONTROL STRATEGIES

As previously delineated, aircraft MG inherently function as autonomous systems in islanded mode [16], [17]. Three principal control paradigms are conceivable: centralized, decentralized, and distributed. The centralized approach is characterized by a singular, powerful controller that performs the management operations of the whole network by minimizing a suitable objective function. In the context of aircraft MG, recent works, such as that outlined in [18], contemplate various generators within the framework of a Virtual Power Plant to establish a centralized control center. In contrast, decentralized control adopts a hierarchical structure, necessitating a robust communication network to facilitate information exchange between the high and low levels within the hierarchy. Centralized and, to a lesser extent, decentralized solutions are prone to faults, require high-bandwidth communications, and are subject to privacy violation issues. The distributed control uses local communication networks for communications only among “adjacent” (in a suitable way) elements of the network. Clearly, both the communication and the computation burden are reduced in the distributed control. Many studies have investigated the design of consensus-based algorithms for the control of distributed MG [19], [20], [21]. For instance, to reduce transmission losses, a distributed control strategy under a directed communication network has been investigated in [22], based on Multi-Agent Systems (MAS). MAS with distributed optimization has been proposed in [23], where a real-time EMS has been designed considering demand and generation as constraints, with robustness to time-varying communication topologies and uncertainties, as in the case of devices addition and removal. The use of consensus-based algorithms [24] is the natural approach in distributed control, and real-time solutions with robust optimization capabilities with respect to random power requests have been proposed in [25]. Also, a decentralized technique for considering both high-level EMS resulting from optimization and low-level, real-time power sharing has been considered [26], by simplifying the problem with a purely distributed approach (with low computational burden). Another possible solution was presented in [27] with a supervisory level based on consensus-based algorithms, resulting in a distributed optimal control approach. In [28], Plug-and-Play decentralized local controllers for Distributed Generation Units (DGU), considered as voltage generators and communicating in real-time on a connected network with consensus filters, were designed. Nevertheless, the work [27] investigates policies based on power sharing rather than current sharing. Furthermore, most of the state-of-the-art works do not take into account the limited capacity of the ESSs, thus neglecting the scenarios where one or more ESSs could discharge completely (or, on the contrary, get fully

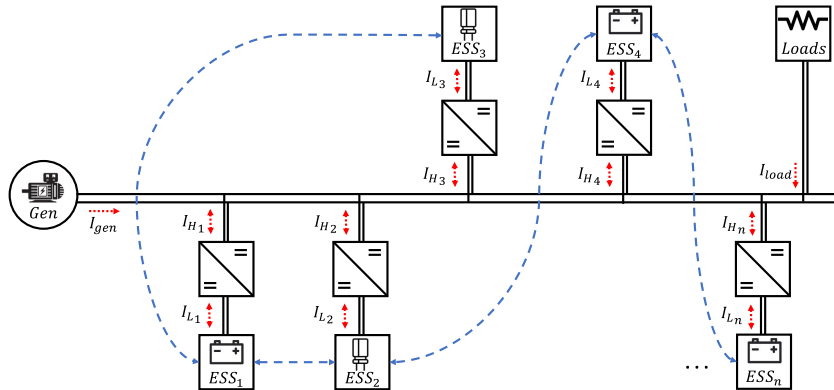


FIGURE 1. Distribution-level microgrid for MEA: main generator feeds avionic loads and multiple ESSs. Dashed blue lines indicate the communication network.

charged). Finally, also low-level control can be considered within the general framework of consensus-based algorithms for the optimization of MG performance. As an example, in [29] a low-level sliding mode controller is considered together with a consensus algorithm to keep the network average voltage at a prescribed level. As in [29] the proposed control strategy aims at reaching consensus among ESS and assumes low-level control based on sliding mode approaches. Currents supplied by each ESS are decided based on the State of Charge (SoC) of each device.

C. MAIN CONTRIBUTION

A major contribution of this work is the development of a SoC-aware consensus-based current sharing algorithm. Unlike conventional consensus-based approaches that focus solely on current sharing without considering the SoC limitations of ESSs, our method dynamically adjusts the current setpoints of each ESS based on its SoC. This allows for a balanced discharge and recharge process across ESSs, ensuring the longevity and safety of the storage units. Specifically:

- Recharging phase (i.e., power absorption): when the ESSs require recharging, a constant current recharge strategy is employed. The proposed consensus algorithm ensures SoC equalization by automatically adjusting the charging current. ESSs with lower SoC are assigned higher current setpoints, facilitating a quicker recharge, while those with higher SoC receive lower setpoints to maintain balance across the system.
- Discharging phase (i.e., power delivery): during power delivery, the algorithm ensures that ESS units contribute to load requirements proportionally to their SoC. ESSs with a higher SoC are tasked with delivering more current, while those with lower SoC deliver less. This proportional current distribution not only ensures efficient load management but also prevents over-depletion of any single ESS, extending the lifespan of the storage units and optimizing overall energy use.
- Safety Constraints: another significant innovation is the integration of safety constraints into the control strategy.

The proposed consensus-based algorithm ensures that the SoC of each ESS is always kept within a predefined safe operational range, which can vary depending on the characteristics of each ESS. This safety feature prevents overcharging or over-discharging, which is crucial in aeronautical applications where reliability and operational safety are paramount.

The proposed algorithm fundamentally differs from existing consensus-based current sharing methods. Most previous approaches assume ESS units can deliver or absorb unlimited power without considering their SoC, leading to potential safety risks or inefficiencies. In contrast, our method incorporates the SoC constraints of each ESS, ensuring that each unit operates within safe limits while still contributing to the overall system's energy demands. This makes the proposed method particularly suitable for applications where energy storage systems have varying capacities and must operate safely over extended periods, as in aeronautic microgrids.

D. OUTLINE

The rest of the paper is organized as follows. In Section II some preliminaries and the problem formulation are presented. In Section III the consensus algorithm designed to manage the ESSs of the aeronautic microgrid is presented and detailed, while insight about parameters tuning is provided in Section IV. Simulation results, showing the effectiveness of the proposed algorithm are presented in Section V, with conclusions given in Section VI.

II. PRELIMINARIES AND PROBLEM FORMULATION

The MEA microgrid can be synthetically represented as shown in Figure 1, where the aircraft generator feeds the main bus with 270 VDC. On the main bus, aside from avionic loads, several energy storage systems, such as auxiliary batteries, supercapacitors, and fuel cells are installed. In order to regulate the power flow to/from the ESSs, DC/DC converters (such as buck, boost, buck-boost converters) are installed to perform as a bridge between the main bus and the ESSs. Each ESS is characterized by a time-varying state of charge, which is indicated hereafter with $\zeta_i(t)$. Referring to Figure 1,

in what follows we indicate with I_{gen} the generator current, with I_{load} the total current absorbed by the loads, while I_{g_i} and I_{L_i} indicate the current entering the i th DC/DC converter from the bus side and the ESS side, respectively. Currents I_{g_i} and I_{L_i} are considered positive when flowing to the ESS, negative otherwise. Regarding the SoC dynamics of each ESS, several SoC estimation methods are available in the literature [30]. However, since the precise estimation of the SoC is not the main focus of this work, here we adopt the classical Coloumb counting method [31], that is the SoC of the i th ESS, indicated with ζ_i , is assumed evolve according to

$$\dot{\zeta}_i(t) = \frac{1}{\theta} I_{L_i}(t), \quad \zeta_i(0) = \zeta_{i0}, \quad (1)$$

where θ and ζ_{i0} are the nominal capacity and the initial SoC of the i th ESS, respectively.

Then, given the above microgrid architecture, the objective is to design a distributed control law that allows the orchestration of the charging and discharging processes of each ESS according to their state of charge. Briefly, when the main generator has enough available power to charge the ESSs, each ESS is allowed to recharge absorbing an amount of current that is inversely proportional to its state of charge. On the contrary, when the ESSs are required to support the generator feeding the connected loads, the prescribed total amount of current required from the ESSs will be autonomously divided among the ESSs according to their state of charge, that is the ESSs with a higher state of charge will provide higher current to the loads. Nevertheless, due to the dislocated distribution of the ESSs onboard the aircraft, a communication network among the ESSs is established to allow the exchange of information among them. The problem of coordinating and balancing several ESS within a microgrid can be effectively addressed by leveraging the principles of MAS. In this context, each ESS is considered an agent of the MAS, which operates independently but can communicate with other agents through a limited communication network. This dislocated configuration, with restricted communication paths, mirrors the decentralized nature of aeronautic grid considered in this work. The process of transforming this control challenge into a consensus problem relies on the concept that all ESS units (agents) must achieve a common objective, that is current sharing with SoC balancing, without requiring direct communication with every other ESS in the system. Instead, each agent shares information only with its immediate neighbors in the communication network, which can be constrained by physical or operational limitations. Such communication network is represented by a connected graph $\mathcal{G} = (\mathcal{V}, \mathcal{E})$, where $\mathcal{V} = \{1, \dots, n\}$ indicates the set of nodes and $\mathcal{E} = \{1, \dots, q\}$ is the set of edges interconnecting the ESSs. In the case where the graph is not strongly connected, the above objectives can still be achieved through a distributed consensus algorithm that exploits the existing communication network. Moreover, while achieving such a consensus policy, in order to preserve the ESSs state of health, it is required to keep the SoC of each ESS within

a safety interval. Hence, the above reasoning and desired behavior can be summarized in the following objectives.

Objective 1: The total current absorbed from or provided by the ESSs must be shared among them proportionally to their generation capacity (proportional current sharing), that is

$$w_i I_{L_i} = w_j I_{L_j}, \quad \forall i, j \in \mathcal{N} \quad (2)$$

where w_i and w_j refer to weighting factors associated with the generation capacity of the ESSs with index i and j , respectively.

Objective 2: The state of charge of each ESS must be always constrained as

$$\zeta_i(t) \in [\zeta_{i \min} - \varepsilon, \zeta_{i \max} + \varepsilon] \quad (3)$$

where $\zeta_{i \min}$ and $\zeta_{i \max}$ are the minimum and maximum allowable values, respectively, for the state of charge of the i th ESS, and ε is a small positive value representing an acceptable tolerance.

The first objective requires the ESSs to charge and discharge according to their generation capacity, i.e., ESSs with higher generation capacity will have to absorb smaller current during the charging process, while they will provide more current during the discharging process. The generation capacity can be in general deduced as a combination of several factor, e.g., the ESS capacity or the ESS state of charge or the ESS temperature. In this work, the SoC only is considered to evaluate the generation capacity. The satisfaction of Objective 1 will allow for equalization of the ESS state of charge despite their initial different generation capacity. The second objective, instead, will enforce a safe range of operation of each ESS.

Considering n ESS devices, in what follows we indicate with $\mathcal{N} = \{1, \dots, n\}$, $\mathcal{M}(t) = \{i \in \mathcal{N} : \zeta_i(t) \in (\zeta_{i \min}, \zeta_{i \max})\}$ with m being its cardinality and $\mathcal{P}(t) = \mathcal{N} \setminus \mathcal{M}(t)$. We denote with \mathcal{G}_i the set of nodes (i.e., the ESSs) connected to the i th ESS by communication lines. Moreover, let $\mathcal{T}_i := \{t_{i,0}, t_{i,1}, t_{i,2}, \dots\}$ be a countable set with $0 < t_{i,0} < t_{i,1} < t_{i,2} < \dots$, which defines the set of strictly increasing sequences of time instants for which $\zeta_i(t_{i,k}) = \zeta_{i \max}$ or $\zeta_i(t_{i,k}) = \zeta_{i \min}$ with $i \in \mathcal{N}$, $k \in \mathbb{N}_0$. Moreover, we define $\mathbf{1}_n = [1 \ 1 \ \dots \ 1]^\top$, $\mathbf{0}_n$ represents the n -dimensional zero column vector, while I_n indicates the $n \times n$ identity matrix. For any vector $z \in \mathbb{R}^n$, $\mathbb{E}[z] = \mathbf{1}^\top z/n$ is the average of the entries of the vector z .

III. ESS CONSENSUS-BASED CONTROL

Given the distributed nature of the microgrid in Figure 1, the control architecture is designed as a hierarchical structure comprising two levels: a supervisory controller that sends current references to the ESS indicating the amount of current requested from or provided to the ESSs; and local controllers, one for each ESS, that implement local control laws guaranteeing that the current of each ESS is regulated to the received current reference. Nevertheless, in order

to reduce the computational burden for the supervisory controller and reduce the exchange of information from and to the supervisory controller, the current sharing policy discussed in the previous section can be implemented as a distributed algorithm among the ESSs. In the following, the considered local control algorithm is briefly discussed and the proposed consensus-based strategy is presented.

A. ESS LOCAL CONTROL

The role of the DC/DC converters in Figure 1 is to regulate the current provided or absorbed by the corresponding ESS. Each converter is regulated by a local controller to guarantee that the corresponding current I_{L_i} reaches a desired reference value, preferably in a given fixed time. In order to achieve this goal, let us define for each converter the following auxiliary variable

$$\sigma_i(t) = \bar{I}_{L_i}(t) - I_{L_i}(t) + \eta_i(t), \quad i \in \mathcal{N}, \quad (4)$$

where \bar{I}_{L_i} is the piecewise constant reference current for the i th ESS, while the term η_i represents a time-varying deviation of the reference \bar{I}_{L_i} from the nominal value. Its definition will be detailed in the next subsection.

In order to guarantee that, after a given transient time, each converter successfully controls its output current to the desired reference, control algorithms guaranteeing fixed-time stability need to be enforced on $\sigma_i(t)$. In this work, the fixed-time terminal sliding mode control presented in [32] is employed to guarantee the existence of $T > 0$ so that $\sigma_i(t) \equiv 0$ for all $t \geq T$, all $i \in \mathcal{N}$, irrespective of the initial condition of each converter, that is

$$I_{L_i}(t) = \bar{I}_{L_i} + \eta_i(t), \quad i \in \mathcal{N}. \quad (5)$$

for all $t \geq T$. Hence, hereafter the dynamics of the closed-loop system will be derived assuming the local controller transient has expired and that (5) holds.

B. ESS CONSENSUS-BASED CONTROL

The consensus policy that allows sharing the available current among the ESSs consists of assigning a nominal current setpoint (\bar{I}_{L_i} , provided by the supervisory control) to each ESS, and then applying a variation through an additional term (computed locally by each ESS) that enforces the consensus among the ESSs. The deviation term of each setpoint is hereafter indicated with $\eta_i(t)$. Specifically, let us define the dynamics of $\eta = [\eta_1, \eta_2, \dots, \eta_n]^\top$ as

$$\dot{\eta}(t) = -(bL(\zeta) + aG(\zeta))\eta(t) - (bL(\zeta)C(\zeta) + aG(\zeta))\bar{I}_L(t), \quad (6)$$

with $\eta(0) = \eta_0$, where $\eta_0 \in \mathbb{R}^n$, $\zeta = [\zeta_1, \zeta_2, \dots, \zeta_n]^\top$, a and b are positive constant scalars and $\bar{I}_L = [\bar{I}_{L_1}, \bar{I}_{L_2}, \dots, \bar{I}_{L_n}]^\top$. Moreover, $L(\cdot)$, $C(\cdot)$ and $G(\cdot)$ are $\mathbb{R}^n \mapsto \mathbb{R}^{n \times n}$ functions with L being the time-varying Laplacian matrix, $C := \text{diag}[c_{11}(\zeta_1), c_{22}(\zeta_2), \dots, c_{nn}(\zeta_n)]$ with $c_{ii} = \zeta_i(0) \text{sign}(\bar{I}_{L_i})$, and $G := \text{diag}[g_{11}(\zeta_1), g_{22}(\zeta_2), \dots, g_{nn}(\zeta_n)]$,

where $g_{ii}(\cdot): \mathbb{R} \rightarrow \mathbb{R}_{\geq 0}$ is a piecewise constant function defined as

$$g_{ii}(s) = \begin{cases} 0 & \text{if } s \in (\zeta_{i \min}, \zeta_{i \max}), \\ 1 & \text{otherwise.} \end{cases} \quad (7)$$

Denoting $\bar{g}_i(s) = 1 - g_{ii}(s)$, the elements of the Laplacian matrix $L(\zeta)$ are instead defined as

$$l_{ij}(\zeta) = \begin{cases} \bar{g}_i(\zeta_i) \sum_{k \in \mathcal{G}_i} \bar{g}_k(\zeta_k) & \text{if } i = j, \\ -\bar{g}_i(\zeta_i)\bar{g}_j(\zeta_j) & \text{if } i \in \mathcal{G}_j, \\ 0 & \text{otherwise,} \end{cases} \quad (8)$$

as (9), shown at the bottom of the next page. Note that the rationale behind the design of the time-varying Laplacian matrix consists of setting the i th row and i th column of L to the null vector when the i th ESS is either fully charged or fully discharged. Nevertheless, when such even occurs, the Laplacian defined in (9) still preserves the null sum of column and row elements.

In the following, for the sake of simplicity, the dependence of all the variables on their arguments will be omitted. Recalling (6), for the i th element of η , it holds that

$$\dot{\eta}_i = - \sum_{j=1}^n (bl_{ij} + ag_{ij})\eta_j - \sum_{j=1}^n (bl_{ij}c_{jj} + ag_{ij})\bar{I}_{L_j}, \quad (10)$$

that is

$$\dot{\eta}_i = \begin{cases} -b \left(\sum_{j=1}^n l_{ij}\eta_j - \sum_{j=1}^n l_{ij}c_{jj}\bar{I}_{L_j} \right) & \text{if } \zeta_i \in (\zeta_{i \min}, \zeta_{i \max}) \\ -a(\eta_i(t) + \bar{I}_{L_i}) & \text{otherwise,} \end{cases} \quad (11)$$

where the first case derives from the definition of G , while the second case follows from the definition of L . Let us provide some insight into the definition of (6). The dynamics of η can be seen as those of a linear parameter-varying system of the form $\dot{\eta} = A(\zeta)\eta + B(\zeta)\bar{I}_L(t)$, where matrices A and B are specifically designed to obtain the desired transient and steady-state behavior, as will be detailed in Theorem 1. More precisely, with reference to (6), the part of $A(\zeta)$ and $B(\zeta)$ that depend on $L(\zeta)$ models the consensus dynamics, while the part that related to $G(\zeta)$ solely takes into account the dynamics of the i th agent. In the following, the main assumptions required for the proposed algorithm are presented.

Assumption 1 (Quick Transient): The parameters a and b are chosen large enough so that the transient dynamics of η_i can be neglected.

Assumption 2 (Initialization of η): The value of $\eta(0)$ is selected such that $\mathbb{1}_n^\top \eta(0) = 0$.

The first assumption suggests that system (1)–(6) have the *two-time-scale* property [33, Chapter 11], where (6) is referred to as the fast model while (1) is the slow model. This is a reasonable assumption since the process of adapting the current setpoint (i.e., the dynamics of η) is much faster than

the dynamics of the ESS state of charge (i.e., the dynamics of ζ).

Regarding the second assumption, the most straightforward choice of the initial state of $\eta_i(0)$ that satisfies Assumption 2 is $\eta(0) = 0_n$. As will be shown in Lemma 2, the consequence of such choice of initial condition is that the average value of the entries of η is preserved and identical to zero when $\zeta_i \in (\zeta_{i \min}, \zeta_{i \max})$ for all $i \in \mathcal{N}$. Note that this is not a strong assumption since the choice of $\eta(0)$ is left to the designer.

Considering the scenario of n ESSs, the consensus-based algorithm (6) with I_{L_i} as in (5), manages to orchestrate the current onboard the aircraft as shown in the following theorem. Hereafter, exploiting Assumption 1, we will say that the i th ESS is in *quasi-steady-state* [33] when the transient of η_i has expired and only the dynamics of ζ_i is left.

Theorem 1: Consider a network of n ESS nodes whose SoC dynamics is defined as in (1). If Assumption 1 and 2 hold, then the consensus law (6) guarantees the following properties:

- 1) *When all the ESS nodes are in quasi-steady-state and $\zeta_i \in (\zeta_{i \min}, \zeta_{i \max})$ for all $i \in \mathcal{N}$, then the proportional current sharing policy is enforced with*

$$I_{L_i}(t) = \mathbb{E}[C\bar{I}_L] + (1 - c_{ii})\bar{I}_{L_i} \quad \forall i \in \mathcal{N}, \quad (12)$$

and the total current absorbed by the ESSs converges to the sum of reference currents, i.e.

$$\sum_{i \in \mathcal{N}} I_{L_i}(t) = \sum_{i \in \mathcal{N}} \bar{I}_{L_i}. \quad (13)$$

- 2) *If the i th ESS reaches either its maximum or minimum allowable SoC, then the corresponding current I_{L_i} tends to zero exponentially with time constant α .*
- 3) *When all the ESS nodes are in quasi-steady-state, then*

$$\begin{cases} I_{L_i}(t) = 0 & \text{if } i \in \mathcal{P}, \\ I_{L_i}(t) = \mathbb{E}[C\bar{I}_L] + (1 - c_{ii})\bar{I}_{L_i} & \text{if } i \in \mathcal{M}, \end{cases} \quad (14)$$

and the total current absorbed by the ESSs is

$$\sum_{i \in \mathcal{N}} I_{L_i}(t) = \frac{m}{n} \sum_{i \in \mathcal{N}} c_{ii}\bar{I}_{L_i} + \sum_{i \in \mathcal{M}} (1 - c_{ii})\bar{I}_{L_i}. \quad (15)$$

In the following, we present several lemmas that will be instrumental in constructing the proof of Theorem 1. Lemma 2 presents the behavior of the ESSs currents and variables η_i when all the ESSs are either charging or discharging. Lemma 3 characterizes the evolution of each η_i and I_{L_i} when the i th ESS is fully charged or discharged. Lemma 4 shows that the average value of $\dot{\eta}$ is preserved in

time while the average value of η converges towards a steady-state value. Finally, Lemma 5 proves that the summation of currents absorbed by the ESSs converges to a given value depending on the consensus policy. For each lemma, it is implicitly assumed that the assumptions of Theorem 1 hold.

Lemma 2: Assume that each ESS node is in quasi-steady-state and $\zeta_i(t) \in (\zeta_{i \min}, \zeta_{i \max})$ for all $i \in \mathcal{N}$. Then

$$\eta_i(t) = \mathbb{E}[C\bar{I}_L] - c_{ii}\bar{I}_{L_i}, \quad (16)$$

and

$$\sum_{i \in \mathcal{N}} I_{L_i}(t) = \sum_{i \in \mathcal{N}} \bar{I}_{L_i}. \quad (17)$$

Proof: Since $\zeta_i(t) \in (\zeta_{i \min}, \zeta_{i \max})$ for all $i \in \mathcal{N}$, then from (6) one has

$$\dot{\eta}(t) = -bL\eta(t) - bLC\bar{I}_L = -bL(\eta(t) + C\bar{I}_L). \quad (18)$$

Consider the state variable translation $z(t) = \eta(t) + C\bar{I}_L$. Then the dynamics of $z(t)$ is

$$\dot{z}(t) = -bLz(t). \quad (19)$$

Since the digraph associated to the Laplacian L is weight-balanced by construction, by [24, Theorem 7.4] $z(t)$ reaches consensus, that is the quasi-steady-state of $z(t)$ is

$$z(t) = \mathbb{E}[z(0)]\mathbb{1}_n. \quad (20)$$

Therefore, reverting to the original variable $\eta(t)$

$$\eta(t) = \mathbb{E}[\eta(0)]\mathbb{1}_n + \mathbb{E}[C\bar{I}_L]\mathbb{1}_n - C\bar{I}_L, \quad (21)$$

and taking into account Assumption 2, (16) holds.

Furthermore, from (16)

$$\sum_{i \in \mathcal{N}} \eta_i(t) = n\mathbb{E}[C\bar{I}_L] - \sum_{i \in \mathcal{N}} c_{ii}\bar{I}_{L_i} = 0, \quad (22)$$

and from (5) we have

$$\sum_{i \in \mathcal{N}} I_{L_i}(t) = \sum_{i \in \mathcal{N}} \bar{I}_{L_i}(t) + \sum_{i \in \mathcal{N}} \eta_i(t). \quad (23)$$

Finally, (17) trivially follows by plugging (22) into (23). \square

Condition (17) indicates that, if the set of ESSs is in quasi-steady-state and all the ESSs are either charging or discharging, the total current provided or absorbed by the ESSs will eventually converge to a fixed value given by the summation of current references (selected by the supervisory control). It must be noted that this result does depend neither on ζ_i , nor on any other parameter of the microgrid.

Remark 1: The consensus is actually performed on the z variable, as all the components of z converge to the same

$$L = \begin{bmatrix} \bar{g}_1(\bar{g}_2 + \dots + \bar{g}_n) & -\bar{g}_1\bar{g}_2 & \dots & -\bar{g}_1\bar{g}_n \\ -\bar{g}_2\bar{g}_1 & \bar{g}_2(\bar{g}_1 + \bar{g}_3 + \dots + \bar{g}_n) & \dots & -\bar{g}_2\bar{g}_n \\ \vdots & \vdots & \ddots & \vdots \\ -\bar{g}_n\bar{g}_1 & -\bar{g}_n\bar{g}_2 & \dots & \bar{g}_n(\bar{g}_1 + \dots + \bar{g}_{n-1}) \end{bmatrix}, \quad (9)$$

value. On the other hand, the variables η_i reach a weighted consensus based on the parameters c_{ii} .

Let us now investigate the behavior of η_i and I_{L_i} when one or more ESSs are fully charged or discharged.

Lemma 3: Assume that each ESS node is in quasi-steady-state and for the i th ESS it holds that $\zeta_i \notin (\zeta_{i\min}, \zeta_{i\max})$. Then

$$\eta_i(t) = -\bar{I}_{L_i}, \quad (24)$$

and

$$I_{L_i}(t) = 0. \quad (25)$$

Proof: The proof trivially follows from the definition of η_i in (11). In fact, in the case of $\zeta_i \notin (\zeta_{i\min}, \zeta_{i\max})$ from (11) we have

$$\dot{\eta}_i(t) = -a(\bar{I}_{L_i} + \eta_i(t)), \quad (26)$$

which yields

$$\eta_i(t) = \eta_i(t_{i,k})e^{-a(t-t_{i,k})} - \bar{I}_{L_i}(1 - e^{-a(t-t_{i,k})})$$

for all $t \geq t_{i,k}$, with $t_{i,k}$ being the time instant when ζ_i leaves the set $(\zeta_{i\min}, \zeta_{i\max})$, thus proving (24) when the i th ESS is in quasi-steady-state. Condition (25) is proved by simply plugging (24) into (5). \square

This lemma proves that, once the i th ESS is fully charged or discharged, the corresponding η_i tends to $-\bar{I}_{L_i}$ to compensate the nominal reference, thus controlling the i th ESS current to zero in order to interrupt the charging or discharging process.

Remark 2: Note that, when charging the ESSs, the proposed strategy implicitly implements the well-known constant current (CC) and constant voltage (CV) charging strategy [34]. In fact, with this strategy, the ESS is initially charged with the CC mode and the ESS voltage (equivalently, the SoC) gradually increases. When the ESS voltage reaches the maximum charge voltage (equivalently, the maximum SoC), the ESS changes its mode from the CC mode charge to the CV mode charge. When setting a constant voltage, the current injected into the ESS decreases exponentially as stated in point 2) of Theorem 1.

In the following, we give a characterization of the average values of $\dot{\eta}$ and η .

Lemma 4: Consider dynamics (6), with $g_{ii}(\cdot)$ defined in (7). When the ESSs are in quasi-steady-state then

$$\mathbb{E}[\dot{\eta}(t)] = 0, \quad (27)$$

$$\mathbb{E}[\eta(t)] = \frac{1}{n} \left[\sum_{i \in \mathcal{M}} (\mathbb{E}[C\bar{I}_L] - c_{ii}\bar{I}_{L_i}) \right] - \frac{1}{n} \sum_{i \in \mathcal{P}} \bar{I}_{L_i}. \quad (28)$$

Proof: Without loss of generality, let us assume that initially $\zeta_i \in (\zeta_{i\min}, \zeta_{i\max})$ for all $i \in \mathcal{N}$. Then, from definition of η in (6) and that of G , it holds that

$$\dot{\eta} = -bL(\eta - C\bar{I}_L). \quad (29)$$

Thus, pre-multiplying on both sides by $\frac{1}{n}\mathbf{1}_n^\top$, we have

$$\frac{1}{n}\mathbf{1}_n^\top \dot{\eta} = \mathbb{E}[\dot{\eta}] = -b\frac{1}{n}\mathbf{1}_n^\top L(\eta - C\bar{I}_L) = 0, \quad (30)$$

where the last equality comes from the definition of the Laplacian matrix in (9). Then $\mathbb{E}[\dot{\eta}(t)] = 0$ for all $t \in [0, t_{i,1})$, where $t_{i,1} := \inf_{t \geq 0} \{t : \zeta_i(t) \notin (\zeta_{i\min}, \zeta_{i\max}), i \in \mathcal{N}\}$.

Furthermore, it is easy to derive from (16) that when the transient of η has expired

$$\begin{aligned} \mathbb{E}[\eta(t)] &= \frac{1}{n} \left[\sum_{i \in \mathcal{N}} (\mathbb{E}[C\bar{I}_L] - c_{ii}\bar{I}_{L_i}) \right] \\ &= \frac{1}{n} (n\mathbb{E}[C\bar{I}_L] - n\mathbb{E}[C\bar{I}_L]) = 0. \end{aligned} \quad (31)$$

If $t_{i,1} = \infty$ (i.e., ESSs are never fully charged or discharged), then the proof is concluded, otherwise if there exists $t_{i,1} < \infty$ such that $\zeta_i(t_{i,1}) \notin (\zeta_{i\min}, \zeta_{i\max})$, then from Lemma 3 η_i exponentially reaches $-\bar{I}_{L_i}$. As a consequence, from (4) it holds that $I_{L_i}(t) = 0$, thus guaranteeing that ζ_i reaches a steady state. This in turn implies that, following from (6), after the transient of η_i has expired, it holds that

$$\begin{aligned} \mathbb{E}[\dot{\eta}] &= \frac{1}{n}\mathbf{1}_n^\top [-bL(\eta + C\bar{I}_L) - aG(\eta + \bar{I}_L)] \\ &= \frac{1}{n}\mathbf{1}_n^\top [-aG(\eta + \bar{I}_L)] \\ &= -\frac{a}{n} \left(\sum_{i \in \mathcal{P}} g_{ii}(\eta_i + \bar{I}_{L_i}) \right) = 0, \end{aligned} \quad (32)$$

where the last equality comes from convergence of η_i towards $-\bar{I}_{L_i}$ for $i \in \mathcal{P}$.

Regarding the convergence of the average value of η , combining together the case of $i \in \mathcal{M}$ from (31) and the case of $i \in \mathcal{P}$ from (24), then the average value of η converges according to (28) where the term in square brackets is not zero unless $\mathcal{M} = \mathcal{N}$. \square

Note that if $\mathcal{M} = \emptyset$, then $\mathcal{P} = \mathcal{N}$, therefore the average value of $\eta(t)$ tends to the average value of the reference vector \bar{I}_L with opposite sign.

In the following lemma, the steady-state value of I_L is investigated.

Lemma 5: Consider dynamics (6), with $g_{ii}(\cdot)$ defined in (7). When the ESSs are in quasi-steady-state then

$$I_L(t) = (I_n - G) \left[\mathbb{E}[C\bar{I}_L]\mathbf{1}_n^\top + (I_n - C)\bar{I}_L \right] \quad (33)$$

for $t \in [t_{i,k}, t_{i,k+1})$ with $t_{i,k}, t_{i,k+1} \in \mathcal{T}_i$, and

$$\sum_{i \in \mathcal{N}} I_{L_i}(t) = \frac{m}{n} \sum_{i \in \mathcal{N}} c_{ii}\bar{I}_{L_i} - \sum_{i \in \mathcal{M}} c_{ii}\bar{I}_{L_i} + \sum_{i \in \mathcal{M}} \bar{I}_{L_i}. \quad (34)$$

Proof: The proof of this lemma is a direct consequence of the results of Lemma 2 and Lemma 3. In fact, due to $I_L = \bar{I}_L + \eta$, it holds that

$$I_{L_i}(t) = 0, \quad (35)$$

if the i th ESS is either fully charged or discharged, and

$$I_{L_i}(t) = \mathbb{E}[C\bar{I}_L] + (1 - c_{ii})\bar{I}_{L_i}, \quad (36)$$

otherwise. Then, from the definition of G and C , (33) directly follows. Moreover, summing all the ESSs currents yields

$$\sum_{i \in \mathcal{N}} I_{L_i}(t) = \sum_{i \in \mathcal{M}} (1 - g_{ii}) \left[\mathbb{E}[C\bar{I}_L] + (1 - c_{ii})\bar{I}_{L_i} \right]$$

$$\begin{aligned}
 &= \sum_{i \in \mathcal{M}} [\mathbb{E}[C\bar{I}_L] + (1 - c_{ii})\bar{I}_{L_i}] \\
 &= \frac{m}{n} \sum_{i \in \mathcal{N}} c_{ii}\bar{I}_{L_i} - \sum_{i \in \mathcal{M}} c_{ii}\bar{I}_{L_i} + \sum_{i \in \mathcal{M}} \bar{I}_{L_i} \quad (37)
 \end{aligned}$$

□

Finally, the proof of Theorem 1 is presented in the following.

Proof of Theorem 1: The proof for Theorem 1 is obtained by combining the results obtained in Lemma 2, Lemma 3, Lemma 4 and Lemma 5. In fact, statement 1) is easily proved by combining the result in (16) with (5); statement 2) is directly proved in Lemma 3; and statement 3) follows from Lemma 5. □

Note that, the actual consensus policy is enforced through the definition of matrix C . In fact, from (33) it can be easily noted that the value of $I_{L_i}(t)$ becomes higher, in absolute value, for either high value $\zeta_i(0)$ and negative \bar{I}_{L_i} (i.e., the case when the i th ESS has high SoC and we want to discharge the ESSs), or for small value of $\zeta_i(0)$ and positive \bar{I}_{L_i} (i.e., the case when i th ESS has low SoC and we want to charge the ESSs). This in turn implies that ESSs with high SoC will provide more current in case of discharge and ESSs with low SoC will absorb more current in case of charge. When the reference current is chosen so that $\bar{I}_{L_i} = \bar{I}_{L_j} = \bar{I}_L^*$, then condition (14) simplifies to

$$\begin{cases} I_{L_i}(t) = 0 & \text{if } i \in \mathcal{P}, \\ I_{L_i}(t) = (\mathbb{E}[C] + 1 - c_{ii})\bar{I}_L^* & \text{if } i \in \mathcal{M}, \end{cases} \quad (38)$$

thus guaranteeing satisfaction of Objective 1 with $w_i = (\mathbb{E}[C] + 1 - c_{ii})^{-1}$. Note that, expressing the ESS SoC in the interval $[0, 1]$ guarantees that w_i is always bounded. Furthermore, it is possible to enforce different consensus policies through different definitions of matrix C . For instance, if one wants to consider a microgrid with ESSs characterized by different power generation capabilities (e.g., depending not only on the SoC of the ESSs but also on the health of each ESS), the consensus policy can be easily modified by designing C so that it will reflect the desired policy.

Finally, it is worth highlighting that, even in the case where not all the ESSs need to be recharged, the proposed algorithm ensures only the ESSs with SoC lower than the maximum allowed value will be charged, while those ESSs that are already fully charged will preserve their SoC. This in turn implies that the consensus-based algorithm presented in Theorem 1 intrinsically eliminates circulating currents, increases efficiency, and reduces battery lifetime degradation. Symmetrically, the same reasoning also holds for the discharging scenario.

IV. REFERENCE AND PARAMETERS TUNING

A. REFERENCE GENERATION AND NODE RECONNECTION

The consensus policy presented in the previous subsections relies on the communication graph described by the laplacian matrix L in (9). According to the definition of L , when the

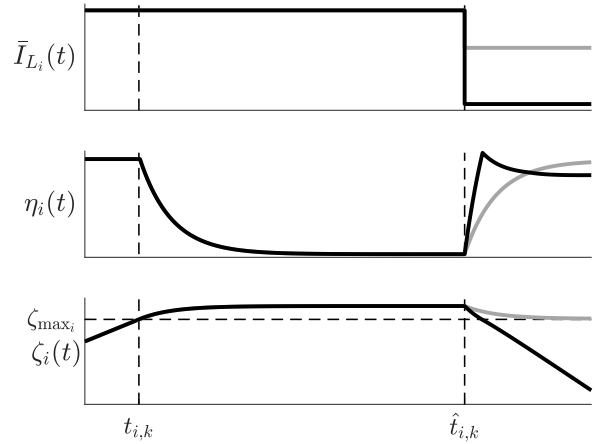


FIGURE 2. Time evolution of I_{L_i} , η_i and ζ_i when condition (43) is satisfied (black lines) and when it is not satisfied (grey lines). When condition (43) is not fulfilled the ESS is not discharged as required.

i th ESS reaches its maximum (or minimum) allowable state of charge, the i th row and column of L are set to zero, hence disconnecting the i th ESS from the communication graph. When this occurs, the dynamics of $\eta_i(t)$ behave according to the second line of (11), thus $\eta_i(t) \rightarrow -\bar{I}_{L_i}$ and $I_{L_i} \rightarrow 0$ to interrupt the charging (or discharging) process. Nevertheless, the ESS current reaches zero exponentially (with time constant a), which implies that the state of charge for the i -th ESS will reach a steady state value slightly above (below, respectively) the provided ζ_{\max_i} (ζ_{\min_i} , respectively). See Figure 2 for a visual representation. When a new setpoint is provided, it must be guaranteed that the dynamics of (11) combined with those of (1) are so that the SoC of the i -th ESS enters again the region $(\zeta_{\min_i}, \zeta_{\max_i})$. As it will be shown shortly, this requirement is not automatically fulfilled unless the new setpoint satisfies some given condition. As the following reasoning symmetrically holds both for the charge and discharge phases, only the case of ESS charging is presented.

Let us indicate with $t_{i,k}$ the time instant when the state of charge of the i th ESS reaches its corresponding ζ_{\max_i} from below. Considering the dynamics of η from (11) and the definition of the of I_{L_i} in (5) it holds that

$$I_{L_i}(t) = (\eta_i(t_{i,k}) + \bar{I}_{L_i}(t_{i,k})) e^{-a(t-t_{i,k})}, \quad \forall t \in [t_{i,k}, \hat{t}_{i,k}), \quad (39)$$

where $\hat{t}_{i,k}$ indicates the time instants when the current reference for the i th ESS is updated after the instant $t_{i,k}$. Then, plugging (39) into (1) it holds that

$$\zeta_i(t) = \zeta_{i \max} + \frac{1}{a\theta} (\eta_i(t_{i,k}) + \bar{I}_{L_i}(t_{i,k})) \left(1 - e^{-a(t-t_{i,k})}\right),$$

for all $t \in [t_{i,k}, \hat{t}_{i,k})$. Hence, the state of charge of the i th ESS will eventually converge to

$$\begin{aligned}
 \zeta_i(\hat{t}_{i,k\infty}) &= \zeta_{i \max} + \frac{1}{a\theta} (\eta_i(t_{i,k}) + \bar{I}_{L_i}(t_{i,k})), \\
 &= \zeta_{i \max} + \frac{I_{L_i}(t_{i,k})}{a\theta}. \quad (40)
 \end{aligned}$$

When, at $t = \hat{t}_{i,k}$, a new current setpoint is provided, η_i will evolve according to (11) (second line) yielding

$$\eta_i(t) = -\bar{I}_{L_i}(\hat{t}_{i,k}) - e^{-a(t-\hat{t}_{i,k})}(\bar{I}_{L_i}(t_{i,k}) - \bar{I}_{L_i}(\hat{t}_{i,k})), \quad (41)$$

for all $t \geq \hat{t}_{i,k}$. Hence, keeping in mind that $I_{L_i}(t) = \bar{I}_{L_i}(\hat{t}_{i,k}) + \eta_i(t)$ for all $t \geq \hat{t}_{i,k}$, plugging $I_{L_i}(t)$ in (1) yields

$$\zeta_i(\check{t}_{i,k\infty}) = \zeta_{i\max} + \frac{\bar{I}_{L_i}(\hat{t}_{i,k}) - \bar{I}_{L_i}(t_{i,k}) + I_{L_i}(t_{i,k})}{a\theta}, \quad (42)$$

where $\zeta_i(\check{t}_{i,k\infty})$ indicates the steady state value reached by ζ_i assuming that no further changes in the current reference occur. Therefore, in order for $\zeta_i(\check{t}_{i,k\infty})$ to enter again in the region $(\zeta_{\min_i}, \zeta_{\max_i})$ the updated current reference must be selected so that

$$\bar{I}_{L_i}(\hat{t}_{i,k}) < \bar{I}_{L_i}(t_{i,k}) - I_{L_i}(t_{i,k}). \quad (43)$$

Note that this is not a restrictive condition. In fact, for instance, when the i -th ESS is fully charged, this condition requires that the updated current reference, which is expected to be negative, cannot be too small in terms of absolute value. Figure 2 shows the evolution of I_{L_i} , η_i and ζ_i both when condition (43) is satisfied and when it is not satisfied. In the first case, after the current reference setpoint is updated, ζ_i enters the region $(\zeta_{\min_i}, \zeta_{\max_i})$ and the i th ESS discharges as required. In the second case, instead, the new current setpoint does not satisfy (43) and the ζ_i never decreases below ζ_{\max_i} . The overshoot of ζ_i when reaching $\zeta_{i\max}$ can be reduced by increasing the time constant a . Nevertheless, it can be noted that condition (43) is required despite the value of a .

Let us now discuss the update of L when one of the ESS nodes fully charges or discharges. The i th row and column of Laplacian matrix (9), depending on the time-variant parameter ζ_i , are set to the null vector when the $\zeta_i \notin (\zeta_{i\min}, \zeta_{i\max})$, which may cause disconnection of nodes of the graph still belonging to the set \mathcal{M} , actually interrupting its consensus. This situation occurs when a graph is weakly connected, and a node has a high degree of centrality. On the contrary, no such difficulty occurs in the case of a strongly connected graph. In fact, in this case, whatever node disconnects, there will always be a path between any two nodes, and consensus is always preserved. If the graph is not strongly connected, we propose hereafter a strategy to re-configuring it. In practice, the proposed algorithm creates alternative paths between connected components of the condensation graph. If a node \mathcal{V}_i reaches its maximum or minimum allowable state of charge, then it is logically disconnected from the graph, in the sense that its information is not used anymore in the consensus-based algorithm (the i th row and column of L are set to the null vector) but the node still exchanges information with its neighbors. If \mathcal{V}_i is a cut-vertex, it may form a no-longer-connected graph. Then, in order to restore the consensus, we generate a condensation graph \mathcal{G}_c with $\mathcal{N} - \mathcal{P}(t)$ vertices. Denote with \mathcal{N}_{C_i} the i th element of the condensation graph and with $v_{i,k}$ the k th node belonging to the i th element of the condensation graph. Next, we connect the elements of the condensation graph

through a connected path, e.g. a simple path. For instance, elements \mathcal{N}_i and \mathcal{N}_j are connected via the nodes $v_{i,k}$ and $v_{j,l}$, exploiting the logically disconnected node. Once the graph has been reconnected appropriately, the L -matrix is updated. The algorithm for re-configuring the graph is synthesized below.

Algorithm 1 Reconfiguration of the Graph

- 1: Node \mathcal{V}_i logically disconnects from \mathcal{G}
 - 2: **if** \mathcal{V}_i is a cut vertex **then**
 - 3: $\mathcal{G}_c = \mathcal{G}(\mathcal{M}(t))$
 - 4: Connect any pair of elements of \mathcal{G}_c
 - 5: Update L
 - 6: **end if**
-

B. PARAMETERS TUNING

The proposed algorithm presents several parameters that can be tuned to obtain the desired performance. As discussed in the previous subsection, with reference to (6), the parameter a can be tuned to increase or decrease the convergence speed of η_i when ζ_i leaves the region $(\zeta_{\min_i}, \zeta_{\max_i})$. When $\zeta_i \in (\zeta_{\min_i}, \zeta_{\max_i})$, then the consensus convergence speed is regulated by the parameter b , as evident from (19). The higher the values of a and b , the faster the convergence of η_i (and thus of I_{L_i}) will be.

Regarding matrix C from (6), let us consider the case when $\bar{I}_{L_i} = \bar{I}_{L_j} = I_L^*$ for all $i, j \in \{1, 2, \dots, n\}$. Then, equation (38) provides insight into how to select parameters c_{ii} . If one chooses all the elements of the matrix C to be identical, i.e., $c_{ii} = c$ for all $i \in \{1, 2, \dots, n\}$, then currents will be equally distributed among the ESS nodes, that is $I_{L_i} = \bar{I}_L^*$ for all $i \in \{1, 2, \dots, n\}$. Otherwise, parameters c_{ii} can be chosen to represent the generation capacity of the ESS nodes.

V. SIMULATION RESULTS

The consensus algorithm presented in Section III has been tested in simulation, in MATLAB Simulink/Simscape environment, in order to assess its correctness and effectiveness. The case of a microgrid with four different ESSs and resistive loads has been considered both for the ESSs charging and discharging scenarios. In both scenarios, it is assumed that a higher level supervisor provides the references \bar{I}_{L_i} to each ESS local controller and it is assumed that the same reference value is sent to each ESS.

TABLE 1. Microgrid and consensus-based algorithm parameters.

V_B	V_E	θ	$\zeta_{1\min}, \zeta_{2\min}$	$\zeta_{1\max}, \zeta_{2\max}$
270 V	28 V	0.3 Ah	0.2	0.9
a	b	R_L	$\zeta_{3\min}, \zeta_{4\min}$	$\zeta_{3\max}, \zeta_{4\max}$
2	80	20 Ω	0.25	0.85

The microgrid and consensus parameters are shown in Table 1, where R_L indicates the total resistance of the connected loads, V_B is the main bus voltage, $\zeta_{i\max}$ and

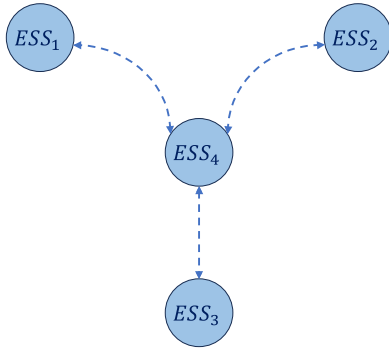


FIGURE 3. Communication network configuration considered in the simulation scenario.

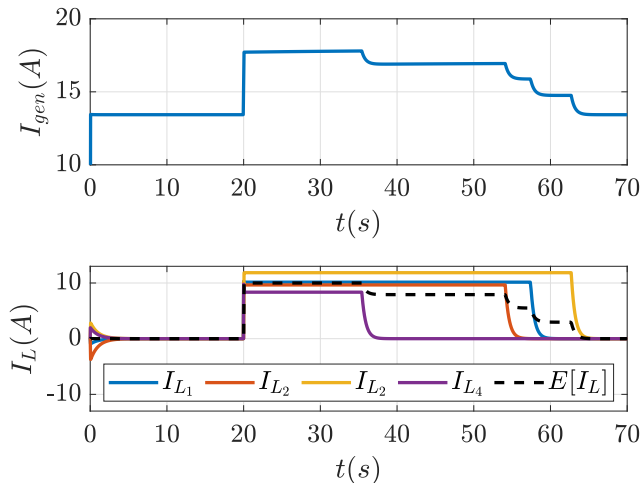


FIGURE 4. Charge scenario. Upper plot: generator current while feeding the loads. Lower plot: time evolution of ESS currents I_{L_i} (solid lines) and $\mathbb{E}[I_L]$ (dashed line).

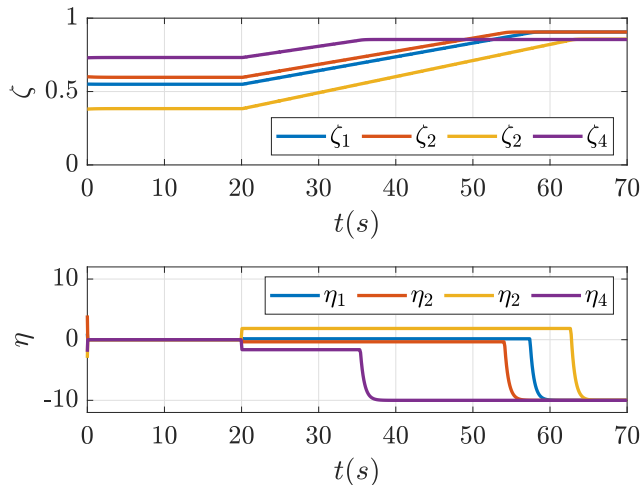


FIGURE 5. Charge scenario. Upper plot: time evolution ζ_i . Lower plot: time evolution of parameter η_i .

$\zeta_{i\min}$ represent the maximum and minimum allowable SoC, respectively, of each ESS. These bounds have been chosen identically for the first and second ESS and for the third and fourth ESS, respectively. Finally, V_E represents the nominal voltage of each ESS. The communication network considered in both simulation scenarios is shown in Figure 3.

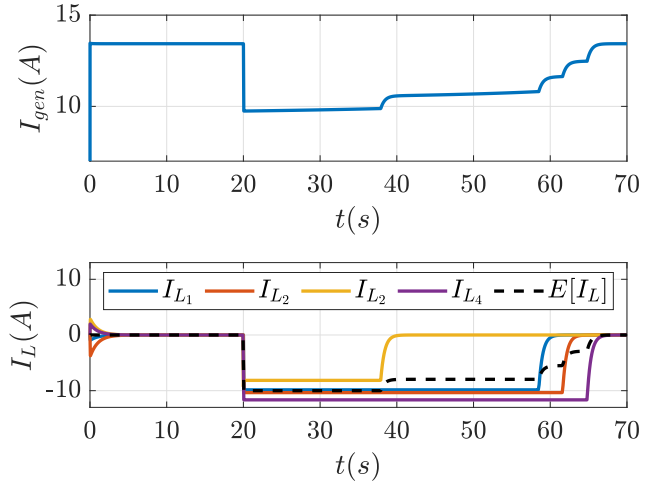


FIGURE 6. Discharge scenario. Upper plot: generator current while feeding the loads with the aid of the ESSs. Lower plot: time evolution of ESS currents I_{L_i} (solid lines) and $\mathbb{E}[I_L]$ (dashed line).

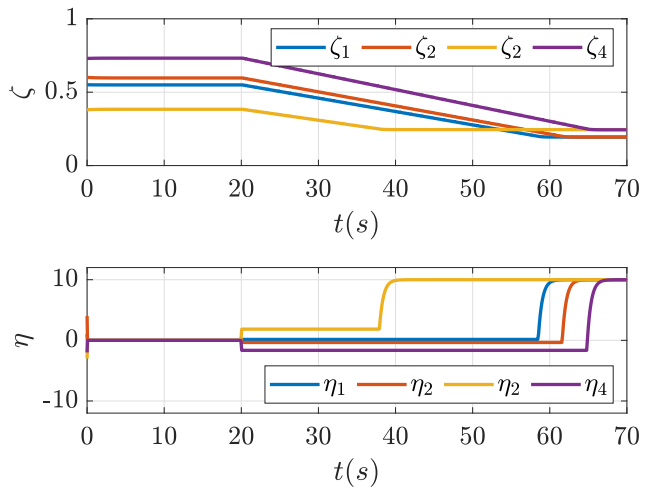


FIGURE 7. Discharge scenario. Upper plot: time evolution ζ_i . Lower plot: time evolution of parameter η_i .

A. CHARGING SCENARIO

In the first scenario, the reference \bar{I}_L sent by the high-level supervisor is initially set to 0 for each ESS. Figure 4 and Figure 5 show that the generator is initially feeding the loads while, accordingly to (12), the ESSs currents are controlled to zero and the SoC remain constant. At 20 s, the external supervisor updates the reference \bar{I}_L to 10 A to allow the ESS to be charged. As shown in Figure 4 and Figure 5, the smaller the SoC of the i th ESS, the higher the corresponding η_i is, thus allowing the ESS with smaller SoC to absorb more current than the others according to (5). Moreover, as suggested by (13) and (14), the average currents I_{L_i} converge to steady-state values around the given reference so that $\mathbb{E}[I_L] = \mathbb{E}[\bar{I}_L] = 10$. At approximately the 37 s, the SoC of the fourth ESS reaches $\zeta_{4\max}$, hence the corresponding η_4 quickly decreases to $-\bar{I}_L$, thus making I_{L_4} decrease to zero. As a natural consequence, the generator current decreases after the fourth ESS is fully charged and the average value of I_L decreases according to (15) (multiply both sides by $1/n$).

Next, as shown in Figure 5, the second, first and third ESS reach full charge at 55 s, 59 s, 65 s, respectively, and the corresponding η_i reach $-\bar{I}_L$ at the same moments.

B. DISCHARGING SCENARIO

The discharging scenario follows similar dynamics to the charging scenario. The reference \bar{I}_L sent by the high-level supervisor is initially set to 0 for each ESS, hence, accordingly to (12) the ESSs currents are set to zero and the SoC remain constant. At 20 s, the higher level supervisor updates the reference \bar{I}_L to -10 A to let the ESS to feed the loads. Symmetrically to the charging case, the consensus algorithm coordinates the ESS so that the ESS with a higher SoC provides more current to the grid. Then, as the second ESS reaches its minimum allowable SoC, its discharge is stopped, and the average value of I_L increases. The rest of the simulation follows with similar behaviors shown for the case of ESS charging.

VI. CONCLUSION

In this paper, a novel consensus-based algorithm for the coordination of multiple ESSs in an aeronautic microgrid is proposed. The presented algorithm automatically changes the predefined current set point of each ESS based on its inherent generation capacity. Considering the SoC as the parameter defining the generation capacity for each ESS, the algorithm assigns a higher current reference to the ESSs characterized by lower SoC. On the other hand, during discharge, a higher current is provided by ESS with higher SoC. Simulation results have shown the effectiveness of the proposed strategy. Future research will move towards the investigation of resilience against loss of communication among the ESSs, electrical failure of one or multiple ESSs or variable generator current limit.

REFERENCES

- [1] R. Lasseter, A. Akhil, C. Marnay, J. Stephens, J. Dagle, R. Guttromson, A. Meliopoulos, R. Yinger, and J. Eto, "White paper on integration of distributed energy resources. The CERTS microgrid concept," *Consortium Electr. Rel. Technol. Solutions*, pp. 1–27, 2002.
- [2] L. E. Zubieta, "Are microgrids the future of energy? DC microgrids from concept to demonstration to deployment," *IEEE Electr. Mag.*, vol. 4, no. 2, pp. 37–44, Jun. 2016.
- [3] J. A. P. Lopes, C. L. Moreira, and A. G. Madureira, "Defining control strategies for microgrids islanded operation," *IEEE Trans. Power Syst.*, vol. 21, no. 2, pp. 916–924, May 2006.
- [4] J. Guanetti, Y. Kim, and F. Borrelli, "Control of connected and automated vehicles: State of the art and future challenges," *Annu. Rev. Control.*, vol. 45, pp. 18–40, Jan. 2018.
- [5] Z. Jin, G. Sulligoi, R. Cuzner, L. Meng, J. C. Vasquez, and J. M. Guerrero, "Next-generation shipboard DC power system: Introduction smart grid and DC microgrid technologies into maritime electrical networks," *IEEE Electr. Mag.*, vol. 4, no. 2, pp. 45–57, Jun. 2016.
- [6] A. Barzkar and M. Ghassemi, "Components of electrical power systems in more and all-electric aircraft: A review," *IEEE Trans. Transport. Electr.*, vol. 8, no. 4, pp. 4037–4053, Dec. 2022.
- [7] A. Cavallo, G. Cancellio, and B. Guida, "Supervised control of buck–boost converters for aeronautical applications," *Automatica*, vol. 83, pp. 73–80, Sep. 2017.
- [8] A. Cavallo, G. Cancellio, B. Guida, P. Kulsangcharoen, S. S. Yeoh, M. Rashed, and S. Bozhko, "Multi-objective supervisory control for DC/DC converters in advanced aeronautic applications," *Energies*, vol. 11, no. 11, p. 3216, Nov. 2018.
- [9] A. Cavallo, G. Cancellio, and A. Russo, "Integrated supervised adaptive control for the more electric aircraft," *Automatica*, vol. 117, Jul. 2020, Art. no. 108956.
- [10] G. Cancellio, A. Cavallo, A. Lo Schiavo, and A. Russo, "Multi-objective adaptive sliding manifold control for more electric aircraft," *ISA Trans.*, vol. 107, pp. 316–328, Dec. 2020.
- [11] A. Cavallo, A. Russo, and G. Cancellio, "Control of supercapacitors for smooth EMA operations in aeronautical applications," in *Proc. Amer. Control Conf. (ACC)*, Jul. 2019, pp. 4948–4954.
- [12] D. Wyatt and M. Tooley, *Aircraft Electrical and Electronic Systems*, 2nd ed., Evanston, IL, USA: Routledge, 2018.
- [13] X. Wang, J. Atkin, N. Bazmohammadi, S. Bozhko, and J. M. Guerrero, "Optimal load and energy management of aircraft microgrids using multi-objective model predictive control," *Sustainability*, vol. 13, no. 24, p. 13907, Dec. 2021.
- [14] H. Yang, "A review of structural batteries implementations and applications," in *Proc. IEEE Transp. Electr. Conf. Expo (ITEC)*, Jun. 2020, pp. 223–228.
- [15] M. P. O'Connell et al., "Airplane-quadcopter UAV hybrid incorporating power regeneration technologies & weight minimization," in *Proc. IEEE Conf. Technol. Sustainability (SusTech)*, Apr. 2022, pp. 154–160.
- [16] L. Fusheng, L. Ruisheng, and Z. Fengquan, *Microgrid Technology and Engineering Application*, L. Fusheng, L. Ruisheng, and Z. Fengquan, Eds., Oxford, U.K.: Academic Press, 2016, pp. 47–67.
- [17] G. Cancellio, A. Cavallo, M. Cucuzzella, and A. Ferrara, "Fuzzy scheduling of robust controllers for islanded DC microgrids applications," *Int. J. Dyn. Control*, vol. 7, no. 2, pp. 690–700, Jun. 2019.
- [18] P. M. Naina and K. S. Swarup, "Double-consensus-based distributed energy management in a virtual power plant," *IEEE Trans. Ind. Appl.*, vol. 58, no. 6, pp. 7047–7056, Nov. 2022.
- [19] T. Morstyn, A. V. Savkin, B. Hredzak, and V. G. Agelidis, "Multi-agent sliding mode control for state of charge balancing between battery energy storage systems distributed in a DC microgrid," *IEEE Trans. Smart Grid*, vol. 9, no. 5, pp. 4735–4743, Sep. 2018.
- [20] J. Hu and A. Lanzon, "Distributed finite-time consensus control for heterogeneous battery energy storage systems in droop-controlled microgrids," *IEEE Trans. Smart Grid*, vol. 10, no. 5, pp. 4751–4761, Sep. 2019.
- [21] K. M. Bhargavi, N. S. Jayalakshmi, D. N. Gaonkar, A. Shrivastava, and V. K. Jadoun, "A comprehensive review on control techniques for power management of isolated DC microgrid system operation," *IEEE Access*, vol. 9, pp. 32196–32228, 2021.
- [22] C. Zhao, J. He, P. Cheng, and J. Chen, "Consensus-based energy management in smart grid with transmission losses and directed communication," *IEEE Trans. Smart Grid*, vol. 8, no. 5, pp. 2049–2061, Sep. 2017.
- [23] M. H. Ullah, B. Babaiahgari, A. Aloseyat, and J.-D. Park, "A computationally efficient consensus-based multiagent distributed EMS for DC microgrids," *IEEE Trans. Ind. Electron.*, vol. 68, no. 6, pp. 5425–5435, Jun. 2021.
- [24] F. Bullo, *Lectures on Network Systems*, 1st ed., Kindle Direct Publishing, 2022. [Online]. Available: <https://fbullo.github.io/lns/>
- [25] D. M. Sobrinho, J. B. Almada, F. L. Tofoli, R. P. S. Leão, and R. F. Sampaio, "Distributed control based on the consensus algorithm for the efficient charging of electric vehicles," *Electr. Power Syst. Res.*, vol. 218, May 2023, Art. no. 109231.
- [26] J. Zhang, B. She, J. C.-H. Peng, and F. Li, "A distributed consensus-based optimal energy management approach in DC microgrids," *Int. J. Electr. Power Energy Syst.*, vol. 140, Sep. 2022, Art. no. 108015.
- [27] Y. Xu and Z. Li, "Distributed optimal resource management based on the consensus algorithm in a microgrid," *IEEE Trans. Ind. Electron.*, vol. 62, no. 4, pp. 2584–2592, Apr. 2015.
- [28] M. Tucci, L. Meng, J. M. Guerrero, and G. Ferrari-Trecate, "Stable current sharing and voltage balancing in DC microgrids: A consensus-based secondary control layer," *Automatica*, vol. 95, pp. 1–13, Sep. 2018.
- [29] M. Cucuzzella, S. Trip, C. De Persis, X. Cheng, A. Ferrara, and A. van der Schaft, "A robust consensus algorithm for current sharing and voltage regulation in DC microgrids," *IEEE Trans. Control Syst. Technol.*, vol. 27, no. 4, pp. 1583–1595, Jul. 2019.

- [30] R. Xiong, J. Cao, Q. Yu, H. He, and F. Sun, "Critical review on the battery state of charge estimation methods for electric vehicles," *IEEE Access*, vol. 6, pp. 1832–1843, 2018.
- [31] F. Codeca, S. M. Savaresi, and G. Rizzoni, "On battery state of charge estimation: A new mixed algorithm," in *Proc. IEEE Int. Conf. Control Appl.*, Sep. 2008, pp. 102–107.
- [32] Z. Liu, X. Lin, Y. Gao, R. Xu, J. Wang, Y. Wang, and J. Liu, "Fixed-time sliding mode control for DC/DC buck converters with mismatched uncertainties," *IEEE Trans. Circuits Syst. I, Reg. Papers*, vol. 70, no. 1, pp. 472–480, Jan. 2023.
- [33] H. K. Khalil, *Nonlinear System* (Pearson Education). Upper Saddle River, NJ, USA: Prentice-Hall, 2002.
- [34] N. Wassiliadis, J. Schneider, A. Frank, L. Wildfeuer, X. Lin, A. Jossen, and M. Lienkamp, "Review of fast charging strategies for lithium-ion battery systems and their applicability for battery electric vehicles," *J. Energy Storage*, vol. 44, Dec. 2021, Art. no. 103306.



identification, and control of vibrating systems, and energy management of power systems for more electric aircraft.

GIACOMO CANCELLO received the Laurea degree (Hons.) from the former Second University of Napoli (currently, University of Campania "Luigi Vanvitelli"), in 2014, discussing the thesis "Identification and Vibration Control for Flexible Structures," advisor Prof. Alberto Cavallo, and the Ph.D. degree in automatic control, discussing the thesis "Sliding Manifold Control in Advanced Aeronautical Applications," in 2018. His research



ANTONIO RUSSO (Member, IEEE) received the bachelor's and master's degrees (summa cum laude) in computer science engineering and the Ph.D. degree in industrial and information engineering from the Università degli Studi della Campania, in 2015, 2017, and 2021, respectively. From January 2019 to June 2019, he was with the Coordinated Science Laboratory, University of Illinois at Urbana-Champaign, USA. From July 2024 to October 2024, he was with the Centro Internacional Franco Argentino de Ciencias de la Información y de Sistemas, Rosario, Argentina. He is currently an Assistant Professor of automatic control with the University of Campania "Luigi Vanvitelli." His research interests include stability analysis of nonlinear switched and hybrid systems, sliding mode control, and control of power systems in the framework of aircraft electrification. Since 2022, he has been a member of the Conference Editorial Board of the European Control Association. He is an Associate Editor of *Franklin Open*.



ALBERTO CAVALLO (Member, IEEE) is currently a Full Professor of automatic control with the University of Campania "Luigi Vanvitelli." He is working on energy management and supervisory control for more electric aircraft applications. He has been the Coordinator and a Principal Investigator of several international research projects on smart control of electric systems for innovative aeronautic applications. He has published more than 120 journal articles and conference papers, and two books, one published by Springer, and the other by Prentice Hall. His research interests deal with many aspects of the theory of automatic control, including robust control techniques with aeronautic and aerospace applications, with parametric and uncertainties and \mathcal{H}_2 and \mathcal{H}_∞ indices, high-order sliding manifold control, active control of sound and vibrations, and modeling and control of smart actuators with hysteresis.

• • •